Int J Adv Manuf Technol (2018) 94:3863–3874
DOI 10.1007/s00170-017-1087-2

ORIGINAL ARTICLE

Development of cutting force prediction model for vibration-assisted slot milling of carbon fiber reinforced polymers

Muhammad Amin[1,2] · **Songmei Yuan**[1] · **Asif Israr**[2] · **Li Zhen**[1] · **Wu Qi**[1]

Received: 5 April 2017 / Accepted: 12 September 2017 / Published online: 26 September 2017

Abstract Carbon fiber reinforced polymers (CFRP) have got rapidly increased applications in aerospace/aircraft and other fields due to their attractive properties of high specific strength/stiffness, high corrosion resistance, and low thermal expansion. These materials have also some challenging properties like heterogeneity, anisotropy, and low heat dissipation. Due to these properties, the issues of excessive cutting forces and machining damages (delamination, fiber pull-out, surface/subsurface defects, etc.) are encountered in machining. The cutting forces are required to be minimized for qualified machining with reduced damages. In this research, a novel cutting force prediction model has been developed for vibration-assisted slot milling. The experimental machining has been carried out on CFRP-T700 composite material. The effective cutting time per vibration cycle and the force of friction have been expressed/calculated. The feasibility of vibration-assisted machining for CFRP composites has also been evaluated. The relationships of the axial and feed cutting forces with machining parameters were investigated. The results have shown the variations below 10% among experimental and corresponding simulation values (from the model) of cutting forces. However, the higher variations have been found in some experiments which are mainly due to heterogeneity, anisotropy, and some other properties of such materials. The developed cutting force model then validated through pilot experiments and found the same results. So, the developed cutting force model is robust and can be applied to predict cutting forces and optimization for vibration-assisted slot milling of CFRP composite materials at the industry level.

Keywords Vibration-assisted slot milling · Cutting force · Prediction model · Carbon fiber reinforced polymers · CFRP-T700 · Machining parameters

1 Introduction and literature review

Carbon fiber reinforced polymer composites have got widely increased applications in aircraft, aerospace, automobile, and other fields due to their attractive properties of high specific strength, high specific stiffness, high corrosion resistance, and low thermal expansion [1, 2]. Especially, the application of such materials in the aircraft industry has increased rapidly up to 50% by weight (Airbus A-380 of 45%, A350XWB 22%, and Dreamliner 787 by 50% by weight) [3].These composite materials are the primary structural materials and used for panels, stringers, and frames of the fuselage to achieve weight reduction for fuel economy [4]. In addition, these materials have also some challenging properties of inhomogeneity, anisotropy, heterogeneity, and low heat dissipation [1, 2]. Due to these properties, the issues like excessive cutting forces, high surface roughness, and machining damages like delamination, fiber pull-out, and matrix burning have been found in machining and required to be minimized for accurate machining. The cutting forces are the main characteristic

Electronic supplementary material The online version of this article (https://doi.org/10.1007/s00170-017-1087-2) contains supplementary material, which is available to authorized users.

✉ Songmei Yuan
yuansm@buaa.edu.cn

[1] School of Mechanical Engineering & Automation, Beijing Engineering Technological Research Center of High-efficient & Green CNC Machining Process and Equipment, Beihang University, Beijing 100191, China

[2] Department of Mechanical Engineering, Institute of Space Technology, Islamabad, Pakistan

parameter for the machining process and are required to be controlled within technical limits for qualified machining of such materials with better surface integrity and reduced machining damages. The mechanics/mathematical models provide more accurate prediction of cutting forces and are applicable for wide range of related parameters as compared to the experimental investigations. Therefore, the cutting force prediction models are the key requirement for controlling the cutting forces. Even, these materials have been tried to design/manufacture near-to-net shapes, but some processes of drilling and milling are unavoidable. The slot milling is necessarily applied if some openings/cavities are required in the part/assembly or to make the proper seat for mating the parts precisely.

The revolution in composite materials has occurred with the development of carbon and boron fibers [5]. Then, various machining technologies have been developed like cutting, grinding, drilling, and milling for brittle materials [6–9]. However, the newly developed materials were found difficult to machine through conventional machining methods [10]. Some nontraditional machining processes have also been developed including abrasive water-jet machining, electric discharge machining, vibration-assisted machining (VAM), and rotary ultrasonic machining and have been applied for improved machining of brittle materials [11–14]. The ultrasonic energy was first applied for material removal process in 1927 by Wood and Loomis [15]. The static ultrasonic machining was found suitable for machining of materials with hardness greater than 40 HRC [16]. However, the ultrasonic machining has limitations of low machining rates and geometrical errors in the machined parts [17–19]. The vibration-assisted machining has been found as the improved machining method.

One-dimensional vibration-assisted machining (1D VAM) and two-dimensional vibration-assisted machining (2D VAM) were first applied in 1950 and 1980, respectively [20, 21]. The most of the research works in this area has been found for drilling and turning of metals. The improved surface quality and reduced tool wear were investigated for vibration-assisted drilling of aluminum 6061-T6, and a cutting force prediction model was developed [22]. The ultrasonic drilling of carbon fiber reinforced polymers (CFRP) was carried out and the reduction of thrust force has been found to be in excess of 60% with lower delamination as compared to conventional drilling [23]. The conventional drilling of CFRP found induced high stresses in the vicinity of the drilled hole along with high thrust force on the tool in comparison with ultrasonically assisted drilling [24].The reduction of thrust force and drilling-induced delamination were found with the ultrasonic drilling of GFRP composites [25]. The kinematic modeling of the vibration-assisted drilling was proposed for aluminum alloy [26]. The reduced tool forces, improved surface finish, and enhanced tool life were then investigated for 1D VAM and 2D VAM of turning process. Also, the ductile regime was found at increased depth for brittle materials [27]. The vibration-assisted turning was carried out for unidirectional CFRP composites and found that the application of ultrasonic vibration in either the cutting or normal direction significantly decreased the cutting forces, minimized the fiber deformation, and facilitated the fiber fracture at the cutting interface and significant improvement in the quality of a machined surface [28]. The ultrasonic vibration-assisted micro end grinding has been carried out for silica glass, and reduction in normal, tangential, and cross-feed direction grinding forces (up to 50%) have been investigated [29]. The few research works have been found for analysis and experimental investigations of milling processes. However, hardly one or two research works were found for modeling of cutting forces. The cutting force model for 2D vibration-assisted micro end milling was developed for the side milling of Al alloy [30]. The modeling and experimental study was carried out for tangential, radial, and axial direction cutting forces for ultrasonic vibration-assisted side milling of titanium alloy [31]. The significant reduction in surface roughness has found for stainless steel and titanium materials with the excitation of the axial mode of vibration in milling process [32]. The reduction in fraying has been found for vibration-assisted slot milling of CFRP composite material [33]. The elliptical vibration-assisted (EVA) machining was investigated as a more effective machining technique in comparison with feed and axial direction vibration-assisted machining of CFRP composite materials [11].The VAM has been found as the effective advanced machining method for improving the process stability and the quality of the machined components [34]. The ultrasonic vibrations were applied for milling of Al alloy with defined geometry tool (face mill with two cutting edges), and lower surface roughness was investigated [35]. The ultrasonic vibration-assisted side milling was carried out by using minimum quantity lubrication for glass-ceramic material and found a reduction in edge-indentation with improved surface morphology [36]. The reduction of cutting forces was observed up to 32% with 2D ultrasonic vibration-assisted milling for aluminum alloy in comparison to conventional milling [37]. The cutting force in feed direction has modeled for vibration-assisted side milling of AISI 420 stainless steel and found reduced cutting forces than conventional side milling process [38].

From the literature review, it was found that the research has mainly carried out on vibration-assisted drilling and turning. However, few research works were found for parametric investigations for vibration-assisted side and face milling. The available research works were found for Al-alloys and other metals. Hardly, one or two research papers are related to cutting force modeling having certain limitations. The cutting force modeling based on vibration-assisted slot milling is not found in literature for metals or composite materials. So, keeping in view the applications and the complex cutting phenomenon for CFRP

composite materials, there is an essential need for the development of cutting force model and experimental investigations for vibration-assisted slot milling for such materials since the excessive cutting forces have adverse effects on the properties of composite materials and are required to be controlled/minimized up to acceptable technical limits.

In this paper, the mechanistic-based model for axial and feed direction cutting forces has been developed for vibration-assisted slot milling of CFRP composites for the first time. The novel approach has been presented to find the effective cutting time and incorporated the force of friction. The machining aspects have been considered for practical machining for acceptable material removal rates. The experiments have been carried out on CFRP-T700 material, and cutting force constants K_1 and K_2 have been found on the basis of experimental results. The cutting force models have then validated through pilot experiments. The relationships of cutting forces with machining parameters have also been investigated.

2 Development of cutting force prediction model

In this research, the vibration-assisted slot milling is applied as the combination of vibration (along axial direction) and the milling process. The grinding process is considered as the more appropriate process for machining of fiber polymer composites because the cutting depth of individual cutting edge is usually smaller than the diameter of the fiber (5–10 μm). However, the grinding process becomes inefficient due to small cutting depths and less material removal rates (MRR). The vibration-assisted machining has shown the improved results because this type of machining methods adds a displacement of micro-scale amplitude with an ultrasonic frequency to the tip motion of a cutting tool [16, 39]. The defined geometry end mill cutter is used which removes the material continuously in the feed direction, and the cutting process is like a conventional milling process because the vibrations have minimum effect in this direction. Along the axial direction, the end mill cutter performs like a hammer (with high-frequency vibrations) which mainly effect on the surface of the material discontinuously. The relationship of the cutting forces and the slot milling process is shown in Fig. 1.

The entry angle (ϕ_{st}) and exit angle (ϕ_{ext}) of the end mill cutter can be expressed as follows:

$$\phi_{st} = \pi - \arccos\left(1 - \frac{a_e}{R}\right) \tag{1}$$

$$\phi_{ext} = \pi \tag{2}$$

where R is the radius of an end mill cutter and a_e is the radial width of cut.

For the slot milling of the workpiece material, $a_e = R$, then, $\phi_{st} = 0$ and $\phi_{ext} = \pi$.

The chip thickness can be represented as follows:

$$a_c = f_z \sin\theta \tag{3}$$

where a_c, f_z, and θ are the un-deformed chip thickness, feed per tooth, and chip angle for the chip, respectively.

2.1 Axial cutting force model

The high-frequency vibrations are being applied along the axial direction (Z-axis) in this research. Therefore, the

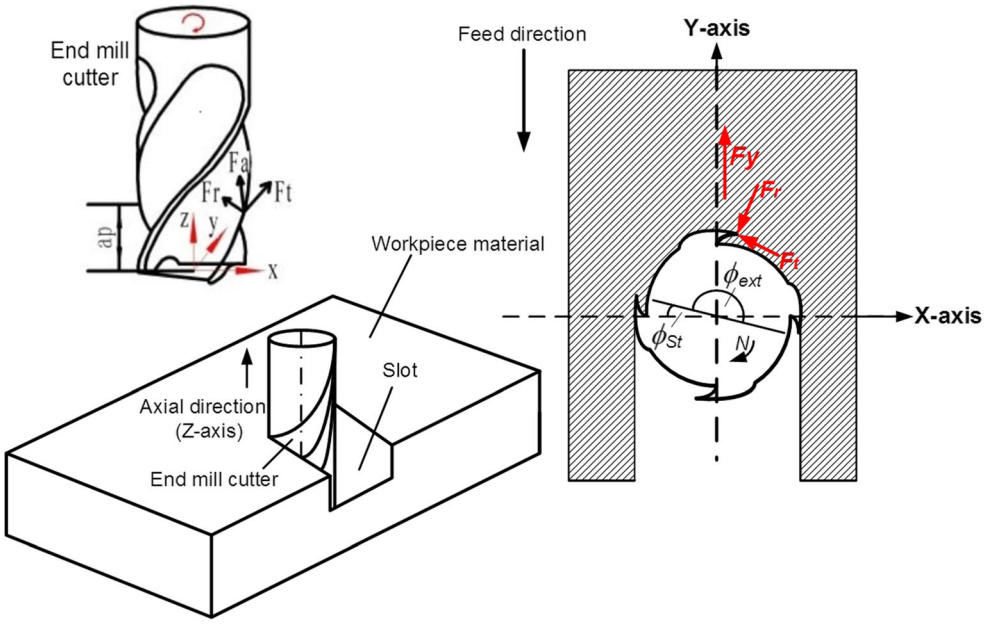

Fig. 1 Illustration of slot milling process and cutting forces

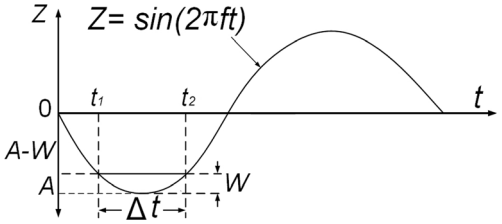

Fig. 2 Relationship for penetration depth (W) and effective cutting time (Δt)

relationship between axial distance Z, frequency f, and amplitude A for sinusoidal wave can be shown as in Fig. 2 and have expressed as follows:

$$Z(t) = A\sin(2\pi ft) \tag{4}$$

The velocity (displacement per unit time), $V(t)$ can be obtained from the derivative of Eq. (4) as under:

$$V(t) = 2\pi Af\cos(2\pi ft) \tag{5}$$

$V(t)$ has units μm/s in Eq. (5), and it can be expressed in units mm/min (same units as feed rate) as under:

$$V(t) = \frac{12\pi Af\cos(2\pi ft)}{100} \tag{6}$$

The effective cutting time, Δt for single sine wave is shown in Fig.2 and can be written as follows:

$$\Delta t = \frac{1}{\pi f}\left[\frac{\pi}{2} - \arcsin\left(1 - \frac{W}{A}\right)\right] \tag{7}$$

where W is the penetration depth of the cutter in sine wave and can be taken as half of the amplitude A (i.e.,$W = \frac{A}{2}$) for simplification. Therefore, Eq. (7) can be simplified as follows:

$$\Delta t = \frac{1}{3f} \tag{8}$$

The feed per tooth, f_z for conventional milling process can be expressed as follows:

$$f_z = \frac{f_r}{Nn_t} \tag{9}$$

where f_r is the feed rate (mm/min) and N (rev/min) is the spindle speed of the end mill cutter.

In vibration-assisted slot milling, both the feed motion and vibratory motion have been found. Since the feed rate, f_r has been applied along feed direction (Y-axis) and displacement per unit time due to ultrasonic vibration is along the axial direction (Z-axis). Therefore, the angle between these two parameters is 90°. Then, the resultant feed rate, f_t can be found through Pythagorean theorem as follows:

$$f_t = \sqrt{(f_r)^2 + \left(\frac{12\pi Af\cos(2\pi ft)}{100}\right)^2} \tag{10}$$

The total feed per tooth, $f_{t,z}$ can be found as follows:

$$f_{t,z} = \frac{\sqrt{(f_r)^2 + \left(\frac{12\pi Af\cos(2\pi ft)}{100}\right)^2}}{Nn_t} \tag{11}$$

By applying Eq.(3), the un-deformed chip thickness a_{cv} can be found for VAM as follows:

$$a_{cv} = \frac{\sqrt{(f_r)^2 + \left(\frac{12\pi Af\cos(2\pi ft)}{100}\right)^2}}{Nn_t}\sin\theta \tag{12}$$

In the milling process, the cutting force is a function of unreformed chip cross-section area. By knowing un-deformed chip thickness, the relationship for axial cutting force can be written as:

$$F = K_1 a_p a_{cv} \tag{13}$$

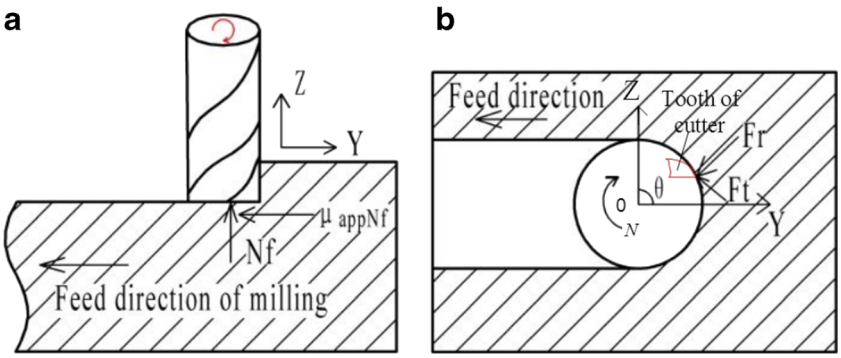

Fig. 3 Illustration for cutting forces and friction force

Table 1 Experimental design

Group	Experiment	Spindle speed, N (rpm)	Feed rate, f_r (mm/min)	Cutting depth, a_p (mm)
1	1–6	2500, 3000, 3500, 4000, 4500, 5000	600	1.0
2	7–11	4500	200, 400, 600, 800, 1000	1.0
3	12–15	4500	600	0.5, 0.75, 1.0, 1.2

where a_p is cutting depth and K_1 is the cutting constant for the axial cutting force. The maximum chip thickness can be found at angle, $\theta = 90°$. Also, the cutting force can be found maximum at this angle ($\theta = 90°$). There is a cycloid movement of the cutter, and two flutes of the cutter remain engaged in cutting, so the total axial cutting force (F_a) can be expressed as follows:

$$F_a = K_1 2a_p \frac{\sqrt{(f_r)^2 + \left(\frac{12\pi A f \cos(2\pi f t)}{100}\right)^2}}{Nn_t} \sin\theta \tag{14}$$

Equation (14) represents the axial cutting force prediction model for vibration-assisted slot milling.

2.2 Feed cutting force model

Since the effect of vibrations in the feed direction is minimum and the machining is just like the conventional slot milling process, therefore the cutting force along feed direction due to a single flute of the end mill cutter is given by:

$$F_{f1} = K_2 \left[F_{feed} + F_{friction}\right] \tag{15}$$

where F_{feed} and F_{friction} are the feed force and friction force for single flute of the end mill, respectively. The relationship for the feed force can be written as follows:

$$F_{f1} = K_2 \left[a_p f_z \sin\theta + \mu_{app} N_F\right] \tag{16}$$

where μ_{app} is the applied friction co-efficient, N_F is the normal cutting force, and K_2 is the cutting force constant. The researcher, Mondelin et al. [40] has defined and reported the value of μ_{app} as follows:

$$\mu_{app} = \mu_{adh} + \mu_{def} \tag{17}$$

The value of μ_{app} is found as 0.10 by considering μ_{adh} is 0.06 and μ_{def} is 0.04 for a dry regime of CFRP material and mono-crystalline diamond conical pin during experiments. The force of friction and the normal force are shown in Fig. 3a, and the radial F_r and thrust force F_t are shown in Fig. 3b. The normal force N_F is the axial cutting force

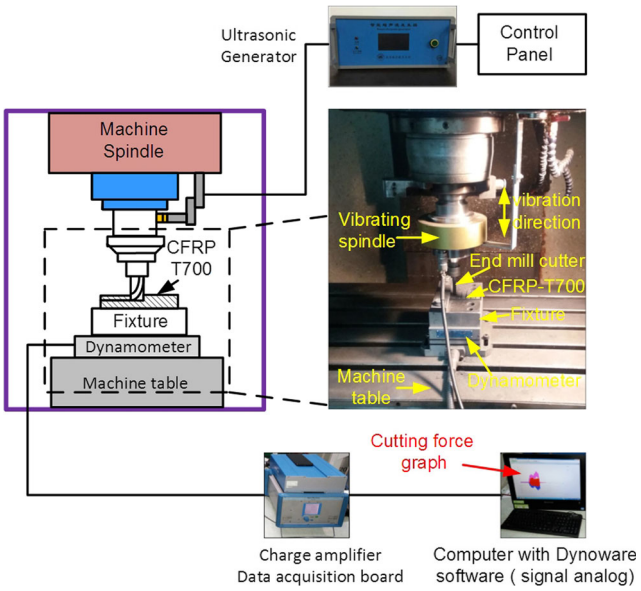

Fig. 4 Experimental setup

Table 2 Properties of machine tool

Nomenclature	Specification
Spindle speed (with ultrasonic device)	0–6000 rpm
Vibration amplitude	10 μm
Vibration frequency	16,000 Hz

Table 3 Mechanical properties of workpiece material

Nomenclature	Specification
Density (ρ)	1.54 g/cm^3
Elastic modulus (E)	7.11 GPa
Tensile strength (TS)	689.08 MPa
Fracture toughness (KIC)	11.5 MPa m$^{1/2}$
Vickers-hardness (Hv)	0.4 GPa
Poisson's ratio (ν)	0.30
Layer configuration	0°, 45°, − 45°, 90°

Table 4 Properties of end mill cutter

Nomenclature	Specification
Diameter	6 mm
No. of flutes	4
Material	CVD-coated carbide
Helix angle	Low helix
Flute length	18
Helix angle	10 deg
Overall length	65 mm

because it is due to the cutter and workpiece combination, so the normal force in case of a single flute is as follows:

$$N_F = K_1 a_p \frac{\sqrt{(f_r)^2 + \left(\frac{12\pi A f \cos(2\pi f t)}{100}\right)^2}}{N n_t} \sin\theta \tag{18}$$

From Eq. (16), the feed force for single flute is given by:

$$F_{f1} = K_2 a_p \left[\frac{f_r + K_1 \mu_{app} \sqrt{(f_r)^2 + \left(\frac{12\pi A f \cos(2\pi f t)}{100}\right)^2}}{N n_t}\right] \sin\theta \tag{19}$$

The maximum chip thickness can be found at angle, $\theta = 90°$, and the cutting force can also be found maximum. There is a cycloid movement of the cutter and two flutes of the cutter remain engaged in cutting. So, the total cutting force can be expressed as follows:

$$F_f = K_2 2 a_p \left[\frac{f_r + K_1 \mu_{app} \sqrt{(f_r)^2 + \left(\frac{12\pi A f \cos(2\pi f t)}{100}\right)^2}}{N n_t}\right] \sin\theta \tag{20}$$

Equation (20) represents the feed cutting force prediction model for vibration-assisted slot milling.

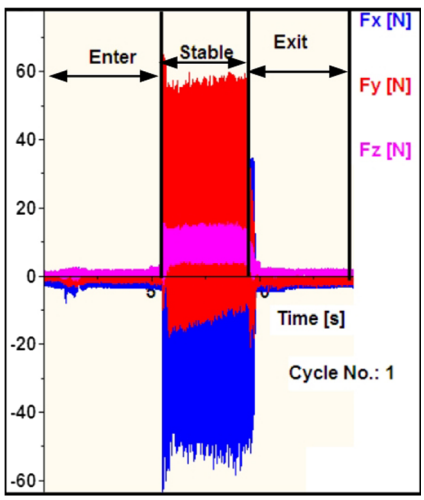

Fig. 5 Cutting force graph for exp. no.5 (N = 4500 rev/min, f_r = 600 mm/min, a_p = 1.0 mm)

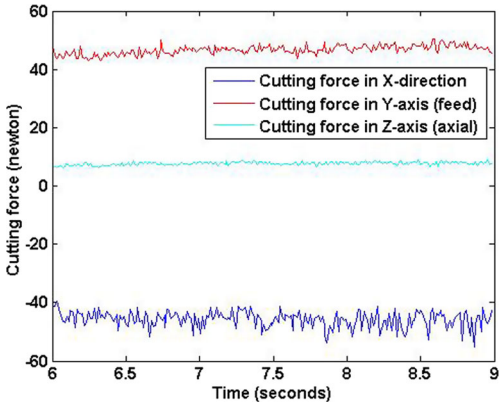

Fig. 6 Measurement of forces for exp. no.5 (N = 4500 rev/min, f_r = 600 mm/min, a_p = 1.0 mm)

3 Experimental setup and conditions

3.1 Experimental design

From the random experiments and the previous studies, the spindle speed, feed rate, and cutting depth are found as essential machining parameters and are considered as variables. Also, the vibration-assisted machining and rotary ultrasonic machining (RUM) were carried out on CFRP-T700 and found that the slot milling of this material (having elastic modulus 7.11 GPa) is feasible/batter with VAM instead of RUM. The significantly higher cutting forces, higher surface roughness, and fraying (one type of material damage in machining) are found in RUM. Moreover, the blockage of the core tool has been observed for RUM. So, the CFRP composites having lower/medium elastic modulus values can be machined accurately through VAM. On the other hand, CFRP composite materials having high elastic modulus (53 GPa) can be machined accurately through RUM as per investigations of Yuan et al. [41]. The experiments have designed by single-factor experiment array three factors. The level of each factor is selected after theoretical calculations, previous experiments,

and keeping in view the higher values of MRR for industrial applications. The experimental design is shown in Table 1.

3.2 Experimental procedure

The experimental setup is shown in Fig. 4. This setup is composed of mainly three parts such as vibration system, CNC vertical machining center, and the end mill cutter. The vibration system has a vibration spindle and vibration generator. The vibration system is capable for high-frequency/ultrasonic vibrations. The CNC vertical machining center (Model: VMC 0850B, Shenyang, China) has fitted with vibration device/attachment (developed by Tianjin University, China) having the vibration spindle. The main specifications of the machine tool are mentioned in Table 2. The workpiece material CFRP-T700 with dimensions 96 × 40 × 5 mm has been used for experimental machining. The single-pass layer-by-layer strategy has been applied for slot milling keeping in view the smooth fracture of carbon fibers of the workpiece material. The mechanical properties of the workpiece material are reported in Table 3. The specifications of the end mill cutter are shown in Table 4. The experiments have been carried out as per experimental design. The cutting force has been measured using the dynamometer (9257B, Kistler, Switzerland). The value of vibration amplitude and vibration frequency has been applied as 10 μm and 16,000 Hz, respectively. These values of amplitude and vibration frequency have been found effective for significant results in the case of CFRP composite materials through previous experiments. The amplitude has been measured with laser Doppler vibrometer (Model: LV-S01, Sunny optical technology, China), and frequency has been noted from the display of the ultrasonic generator.

Table 5 Experimental and simulated data of axial cutting force

Exp. no.	N (rev/min)	f_r (mm/min)	a_p (mm)	Axial force ($F_{a(m)}$) (newton)	Axial force ($F_{a(s)}$ without K_1) (newton)	Axial force ($F'_{a(s)}$ with K_1) (newton)
1	2500	600	1.0	13.779	0.1206	13.989
2	3000	600	1.0	10.137	0.1005	11.657
3	3500	600	1.0	10.042	0.0861	9.987
4	4000	600	1.0	8.031	0.0754	8.746
5	4500	600	1.0	7.727	0.0670	7.771
6	5000	600	1.0	8.432	0.0603	6.994
7	4500	200	1.0	7.614	0.0432	5.011
8	4500	400	1.0	8.154	0.0449	5.208
9	4500	600	1.0	8.556	0.0670	7.771
10	4500	800	1.0	10.090	0.0891	10.335
11	4500	1000	1.0	10.452	0.1113	12.910
12	4500	600	0.5	4.178	0.0335	3.885
13	4500	600	0.75	6.707	0.0503	5.834
14	4500	600	1.0	8.325	0.0670	7.771
15	4500	600	1.2	9.716	0.0804	9.326

4 Experimental results and discussion

The experimental machining process has been divided into three stages, i.e., Enter, Stable, and Exit as shown in Fig. 5. The cutting force data for the stable stage is obtained from the real time cutting force data obtained through Dynoware software (V2.41) in graphical form. The graphical cutting force data then transformed to numerical values of cutting forces by using developed

Table 6 Experimental and simulated data of feed cutting force

Exp. no.	S (rev/min)	f_r (mm/min)	a_p (mm)	Feed force ($F_{f(m)}$) (newton)	Feed force ($F_{f(s)}$ without K_2) (newton)	Feed force ($F'_{f(s)}$ with K_2) (newton)
1	2500	600	1.0	63.226	13.1733	74.112
2	3000	600	1.0	58.978	11.8111	66.449
3	3500	600	1.0	51.272	10.1238	56.956
4	4000	600	1.0	50.687	8.8583	49.836
5	4500	600	1.0	46.636	7.8741	44.299
6	5000	600	1.0	52.824	8.0867	45.495
7	4500	200	1.0	37.950	7.7955	43.857
8	4500	400	1.0	45.570	7.8305	44.054
9	4500	600	1.0	50.830	7.8741	44.299
10	4500	800	1.0	62.842	8.9260	50.217
11	4500	1000	1.0	64.858	10.0863	56.745
12	4500	600	0.5	28.204	2.9852	16.794
13	4500	600	0.75	35.301	4.4417	24.989
14	4500	600	1.0	44.295	7.8741	44.299
15	4500	600	1.2	51.085	11.0026	61.900

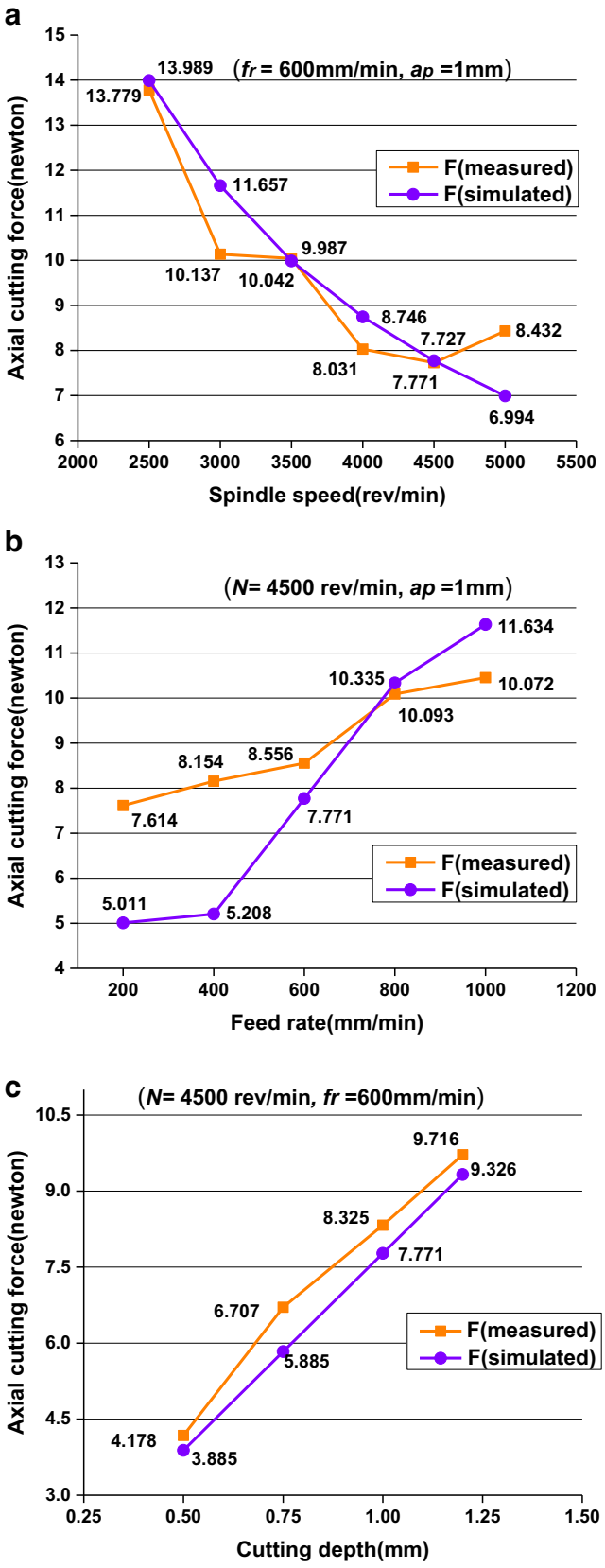

Fig. 7 Axial cutting force and machining parameters

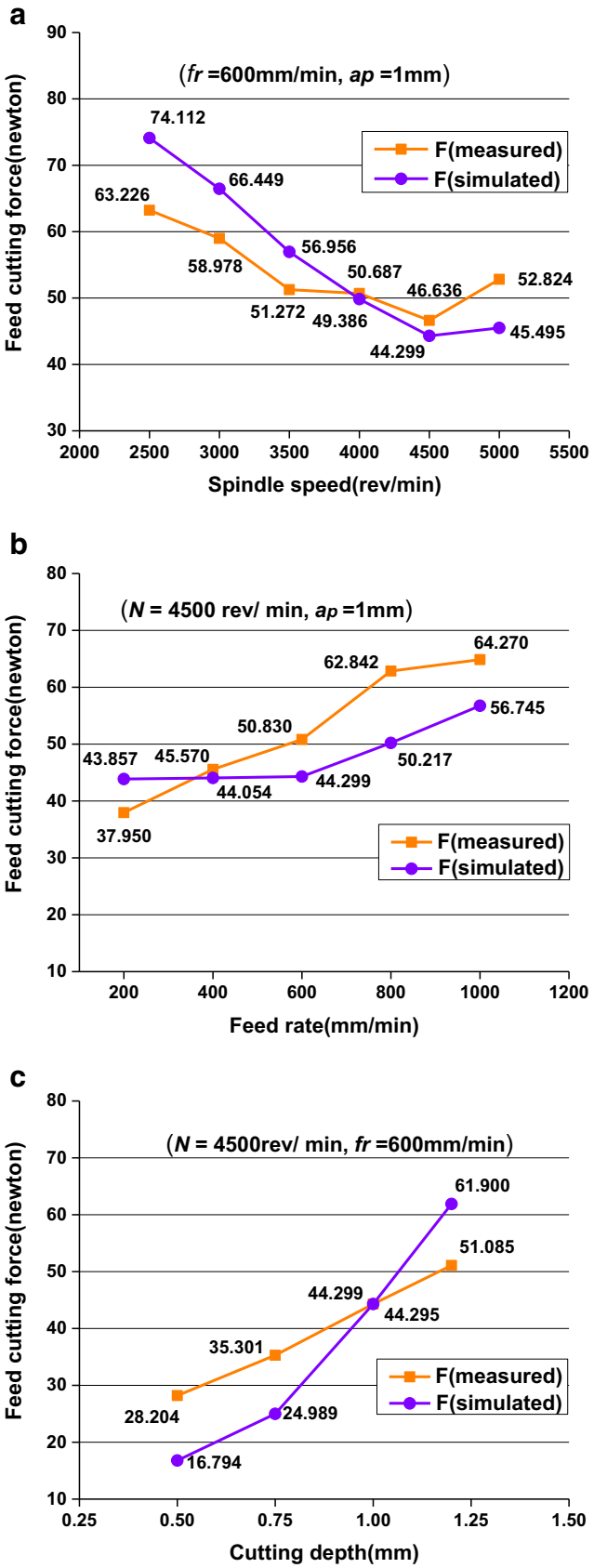

Fig. 8 Feed cutting force and machining parameters

Table 7 Experimental and simulated data of axial cutting force

Exp. no.	N (rev/min)	f_r (mm/min)	a_p (mm)	Axial force ($F_{a(m)}$) (newton)	Axial force ($F_{a(s)}$ without K_1) (newton)	Axial force ($F'_{a(s)}$ with K_1) (newton)	Variations $\frac{\left(F'_{a(s)}-F_{a(m)}\right)}{F_{a(m)}}\times 100\%$
1	3000	400	0.6	6.156	0.0505	5.857	− 4.85
2	3000	400	0.6	6.672	0.0505	5.857	− 12.21
3	3000	600	0.6	8.138	0.0603	6.994	− 14.05
4	3000	600	0.6	7.040	0.0603	6.994	− 0.65
5	3000	600	1.0	13.334	0.1105	12.817	− 3.87
6	3000	600	1.0	12.875	0.1105	12.817	− 0.45
7	3000	400	1.0	9.978	0.0778	9.024	− 9.56
8	3000	400	1.0	9.810	0.0778	9.024	− 8.01
9	4000	400	0.6	4.989	0.0403	4.674	− 6.31
10	4000	400	0.6	4.516	0.0403	4.674	+ 3.49
11	4000	400	1.0	6.581	0.0506	5.869	− 10.81
12	4000	400	1.0	6.984	0.0506	5.869	− 15.96
13	4000	600	0.6	5.021	0.0452	5.243	+ 4.22
14	4000	600	0.6	4.856	0.0452	5.243	+ 7.76
15	4000	600	1.0	9.336	0.0788	9.140	− 2.27
16	4000	600	1.0	9.721	0.0788	9.140	− 6.14

MATLAB code (Fig. 6). The cutting force value obtained through MATLAB code for each force (F_x, F_y, and F_z) is the mean value of all the peak values of the cutting force in the stable stage. The cutting force values obtained by considering peak values are the factual presentation of the cutting force and higher than simply the average values of

Table 8 Experimental and simulated data of feed cutting force

Exp. no.	N (rev/min)	f_r (mm/min)	a_p (mm)	Feed force ($F_{f(m)}$) (newton)	Feed force ($F_{f(s)}$ without K_2) (newton)	Feed force ($F'_{f(s)}$ with K_2) (newton)	Variations $\frac{\left(F'_{f(s)}-F_{f(m)}\right)}{F_{f(m)}}\times 100\%$
1	3000	400	0.6	24.715	4.2445	23.879	− 3.38
2	3000	400	0.6	24.467	4.2445	23.879	− 2.40
3	3000	600	0.6	30.024	5.2760	33.023	+ 9.98
4	3000	600	0.6	41.936	5.2760	33.023	− 21.25
5	3000	600	1.0	55.657	10.8111	61.073	+ 9.73
6	3000	600	1.0	64.280	10.8911	61.073	− 4.98
7	3000	400	1.0	46.627	8.7458	49.203	+ 5.52
8	3000	400	1.0	45.950	8.7458	49.203	+ 7.07
9	4000	400	0.6	18.555	3.1834	17.909	− 4.35
10	4000	400	0.6	20.075	3.1834	17.909	− 10.78
11	4000	400	1.0	41.473	8.0093	45.063	+ 8.65
12	4000	400	1.0	40.046	8.0093	45.063	+ 12.52
13	4000	600	0.6	26.931	4.2070	23.668	− 12.11
14	4000	600	0.6	27.541	4.2070	23.668	− 14.06
15	4000	600	1.0	54.794	8.8583	49.836	− 9.87
16	4000	600	1.0	54.092	8.8583	49.836	− 7.86

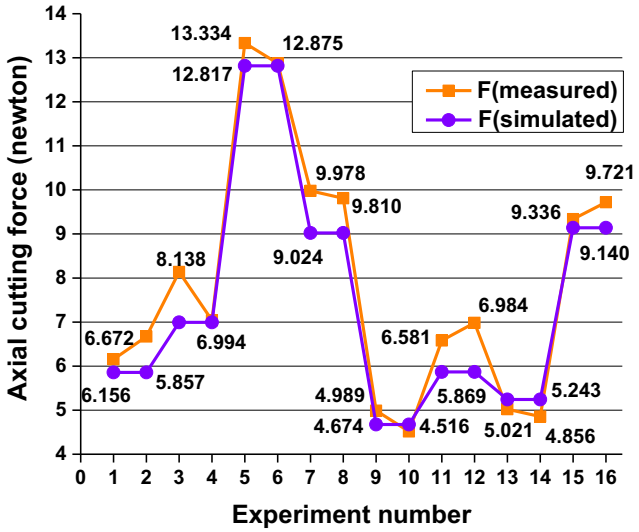

Fig. 9 Comparison of measured and simulated axial force

the cutting forces. The experimental data is recorded in column 5 of Table 5 for the axial force and column 5 of Table 6 for the feed force.

4.1 Obtaining of cutting force constants, K_1 and K_2

The simulation values of the axial cutting force are closest to measurement values when the factor $\sum(F_a - K_1 \times F'_S)^2$ got the minimum value. The linear least square method is applied for this purpose which defines the best fit function with minimizing the error/residual, s as follows [42]:

$$s = \sum_{i=1}^{i=n} (y_i - (ax_i + b))^2 \tag{21}$$

where a and b are constants, y_i and x_i are the dependent and independent variables, respectively, and i is the series of measurements, i.e., $i = 1, 2, 3, 4\ldots n$.

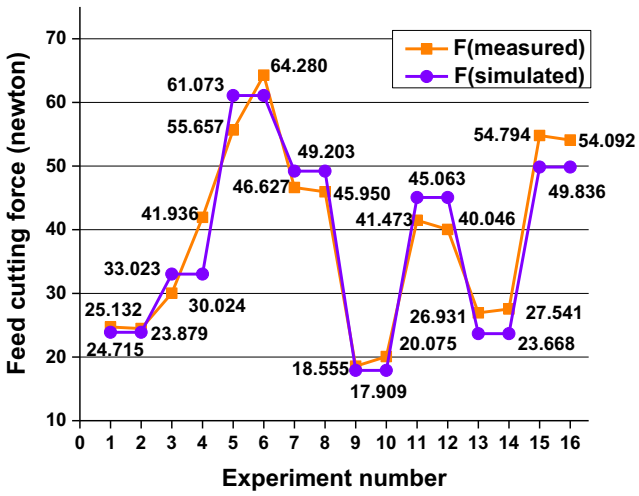

Fig. 10 Comparison of measured and simulated feed force

For minimizing the residual s, the function is then partially differentiated with respect to constants (a and b). The same method has applied to find the value of K_1 by partially differentiating the factor $\sum(F_{a(m)} - K_1 \times F_{a(s)})^2$ with respect to K_1 as follows:

$$\sum 2 \cdot \left(F_{a(m)} - K_1 \times F_{a(s)}\right)\left(-F_{a(s)}\right) = 0 \tag{22}$$

By putting the values of experimental and simulated cutting forces for each experiment, summation of all the experiments and equating to zero, then the value of K_1 is obtained. This value gives the relationship between K_1 and machining parameters. This cutting force constant is based on the relationship of the workpiece material and properties (geometry, material, etc.) of cutting tool and is not dependent on the machining parameters. The same considerations are applied on the factor $\sum(F_{f(m)} - K_2 \times F_{f(s)})$ for feed cutting force model. The values of K_1 and K_2 are found as 115.997 and 5.626, respectively. The data obtained by applying the developed cutting force model for the axial and the feed forces are shown in column 6 of Table 5 and Table 6, respectively.

The axial and the feed cutting force data obtained through experiments and by applying the respective cutting force models have been plotted as shown in Fig. 7 and Fig. 8, respectively. The simulated values of the axial and the feed cutting forces are found to have close match with the measured values of both type cutting forces. These graphs also show that the axial force decreases with the increase of spindle speed. The feed cutting force has found to increase with the increase of spindle speed up to certain limits and then found to decrease. It is pertinent to mention that the significant results have obtained with spindle speed 4500 rev/min. With spindle speed higher than this value, the axial and feed cutting forces are going to increase. This increase in the cutting forces is due to the reason that with higher rotations of the cutter beyond the certain values, the effect of vibrations is found reduced. Both of these forces have found to increase with the increase of feed rate and cutting depth.

The graphical analysis has shown that the simulated values of axial cutting force have a close match (nearly equal) with the measured values of axial cutting forces while the variations of experimental and simulated feed forces found higher. These higher variations are due to the facts that high-frequency vibrations are applied only in the axial direction and also due to inhomogeneity, heterogeneity, anisotropy, and varying thermal behavior of CFRP composites. The variations can rise due to uneven material properties and dislocations of fibers during machining. The value of instantaneous cutting force may change more than three times because when machining different cutting area, the average cutting force may change. So, the error was recorded in some of the cases

and is expected to the acceptable level as per nature of such materials.

Zarchi et al. [38] have developed the cutting force model for vibrations along feed direction (Y-axis) of side milling of AISI 420 stainless steel. However, the effective cutting time for vibration cycle is not calculated and there are issues in the practical application of this model. The cutting force model developed in this paper has the expression for the calculation of the value of effective cutting time for one vibration cycle. The practical aspects of machining have been incorporated in this research by considering cutting angle from 0 to π degrees, maximum chip thickness at angle 90°, and two flutes perform the cutting action in the case of four-fluted end mill. The developed cutting force model for the axial and the feed cutting forces are novel with practical machining requirements.

The maximum values of spindle speed, feed rate, and cutting depth ($N = 5000$ rpm, $f_r = 1000$ mm/min, and $a_p = 1.2$ mm) have been applied to develop the cutting force model. Also, the higher values of machining parameters are significant to increase the MRR as, MRR = $f_r a_p a_e$.

4.2 Validation of cutting force model

The additional experiments were carried out for validation of the developed cutting force model. These pilot experiments have designed three factors, two-level factorial designs and each experiment was repeated. The changed values (from values mentioned in Table 4) of machining parameters have been applied for validation of the cutting force models. The related data is reported in Table 7 and Table 8 and is plotted as shown in Fig. 9 and Fig. 10. From the graphical analysis, it is found that the most of the data points are closely match for the measured and simulated values of cutting forces. Numerically, the variation more than 10% is found in four experiments (exp. 2 as 12.21%, exp. 3 as 14.21, exp.11 as 10.81%, and exp.12 as 15.96%) for the axial cutting force. The variations more than 10% are found in five experiments (exp. 4 as 21.25%, exp. 10 as 10.78%, exp. 12 as 12.52%, exp. 13 as 12.11%, and exp. 14 as 14.06%). These variations show the similar behavior of higher variations for CFRP composites and have supported the findings that variations in cutting force values may occur in cutting forces due to heterogeneity, anisotropy, and other factors mentioned in above discussion. So, the developed axial and feed cutting force models are accurate and can be applied for the prediction of these cutting forces.

5 Conclusions

From the development of cutting force prediction model for the axial and the feed forces and vibration-assisted slot milling of CFRP composite materials, the following conclusions have been drawn:

1. The cutting force prediction model for axial and feed force has been developed for vibration-assisted slot milling of CFRP-T700 composite materials. The graphical/numerical analysis has shown that the measured and the simulated values of cutting forces have a close match (nearly equal), and the variations among their corresponding values are found less than 10% in most of the experimental groups. However, in some cases, higher variations have been found which are due to the heterogeneity, anisotropy, and some other properties of such materials.
2. The developed cutting force model is novel and robust. This model is in the form of one equation and can be applied with ease in calculations. The practical aspects of machining have incorporated in this research by considering cutting angle from 0 to π degrees, maximum chip thickness at angle 90°, and two flutes perform the cutting action at the same time in the case of four-fluted end mill cutter.
3. The significantly higher values of machining parameters have been applied ($N = 5000$ rev/min, $f_r = 1000$ mm/min, and $a_p = 1.2$ mm) for the first time in order to maintain MRR and to close the research work with practical machining. The axial force has been found to decrease with the increase of spindle speed. The feed cutting force has been found to decrease with the increase of spindle speed up to certain limits and then found to increase. Both of the forces (axial and feed force) have been found to increase with the increase of feed rate and cutting depth.

The developed cutting force model for axial and feed force in this paper is applicable for prediction/minimizing of the cutting forces for vibration-assisted slot milling of CFRP composites at the industry level. The input resources can be saved/optimized with the increase of process efficiency and quality of the product.

Acknowledgements This research is financially supported by National High Technology Research and Development Program of China under program no. 863 with grant no.2013AA040105. The authors are indebted to this financial support to accomplish this research work.

References

1. Jones RM (1999) Mechanics of composite materials, 2nd edn. Taylor & Francis Inc, Philadelphia
2. Kaw AK (2006) Mechanics of composite materials, 2nd edn. Taylor & Francis Group, Florida
3. Walz M (2006) The dream of composites. www.rdmag.com. Accessed 5 Jan 2017
4. Saoubi RM, Axinte D, Soo LS, Nobel C, Attia H, Kappmeyer G, Engin S, Sim W (2015) High performance cutting of advanced aerospace alloys and composite materials. CIRP Ann Manuf Technol 64:577–580

5. Ashby MF, Bush SF, Swindells N, Bullough R, Ellison G, Lindblom Y, Cahn RW, Barnes JF (1987) Technology of the 1990s: advanced materials and predictive design [and discussion]. Phil Trans R Soc Land A 322(1567):393–407
6. Sheikh-Ahmad JY (2009) Machining of polymer composites. Springer Science, New York. https://doi.org/10.1007/978-0-387-68619-6
7. Liu JW, Baek DK, Ko TJ (2014) Chipping minimization in drilling ceramic materials with rotary ultrasonic machining. J Adv Manuf Technol 72(9–12):187–190
8. Kalla D, Sheikh-Ahmad J, Twomey J (2010) Prediction of cutting forces in helical end milling of fiber reinforced polymers. Int J Mach Tools Manuf 50:882–891
9. Chen ST, Jiang ZH, Wu YY, Yang HY (2011) Development of a grinding–drilling technique for holing optical grade glass. Int J Mach Tools Manuf 51(2):95–103
10. Groover MP (2010) Fundamental of modern manufacturing: materials, processes, and systems, 4th edn. Wiley & Sons Inc, USA
11. Xu W, Zhang LC, Wub Y (2014) Elliptic vibration-assisted cutting of fiber-reinforced polymer composites: understanding the material removal mechanisms. J Compos Sci Technol 92:103–111
12. Pei ZP, Ferreira PM, Haselkorn M (1995) Plastic flow in rotary ultrasonic machining of ceramics. J Mater Process Technol 48(1): 771–777
13. Lau WS, Wang M, Lee WB (1990) Electric discharge machining of carbon fibre composite materials. Int J Mach Tools Manuf 30(2): 297–308
14. Alberadi A, Artaza T, Suarez A, Rivero A, Girot F (2016) An experimental study on abrasive water jet cutting on CFRP/TiA14V stacks for drilling operations. Int J Adv Manuf Technol 86:691–704
15. Singh RP, Singhal S (2016) Rotary ultrasonic machining: a review. J Mater Manuf Process 31:1795–1824
16. Thoe TB, Aspinwall DK, Wise MLH (1998) Review on ultrasonic machining. Int J Mach Tools Manuf 38(4):239–255
17. Kataria R, Kumar J, Pabla BS (2016) Experimental investigation and optimization of machining characteristics in ultrasonic machining of WC-Co composite using GRA method. J Mater Manuf Process 31:685–693
18. Halm R, Schulz P (1993) Ultrasonic machining of complex ceramic components. Erosion AC Report, DKG 70 70 (6):6–13
19. Gilmore R (1991) Ultrasonic machining–a case study. J Mater Process Technol 28(1–2):139–148
20. Moriwaki T, Shamoto E, Inoue K (1991) Ultraprecision ductile cutting of glass by applying ultrasonic vibration. CIRP Ann Manuf Technol 41(1):559–562
21. Isaev A, Anokhin V (1961) Ultrasonic vibration of a metal cutting tool. Vest Mashinos 41 (Translation from Russian)
22. Zhang SSF, Bone GM (2009) Thrust force model for vibration-assisted drilling of aluminum 6061-T6. Int J Mach Tools Manuf 49:1070–1076
23. Makhdum F, Jennings LT, Roy A, Silberschmidt VV (2012) Cutting forces in ultrasonically asssited drilling of carbon fiber reinforced plastics. J Phys Conf Ser 382:12–19. https://doi.org/10.1088/1742-6596/382/1/012019
24. Phadnis VA, Makhdum F, Roy A, Silberschmidt VV (2012) Experimental and numerical investigations in conventional and ultrasonically assisted drilling of CFRP laminates. Procedia CIRP 1: 455–459
25. Mehbudi P, Baghlani V, Akbari J, Bushrao AR, Mardi NA (2013) Applying ultrasonic vibration to decrease drilling-induced delamination in GFRP laminates. Procedia CIRP 6:577–582
26. Ladonne M, Cherif M, Landon Y, Navez JK, Cahuc O, Castelbajac CD (2015) Modelling the vibration-assisted drilling process: identification of influential phenomena. Int J Adv Manuf Technol 81: 1657–1666
27. Brehl DE, Dow TA (2008) Review of vibration-assisted machining. Precis Eng 32(3):153–172
28. Xu W, Zhang LC (2014) On the mechanics and material removal mechanisms of vibration-assisted cutting of unidirectional fiber-reinforced polymer composites. Int J Mach Tools Manuf 80-81:1–10
29. Hua ZJ, Yan Z, Qiang TF, Shuo Z, Shen GL (2015) Kinematics and experimental study on ultrasonic vibration-assisted micro end grinding of silica glass. Int J Adv Manuf Technol 78:1893–1904
30. Ding H, Chen SJ, Cheng K (2010) Two-dimensional vibration-assisted micro end milling: cutting force modelling and machining process dynamics. Proc IMechE B J Eng Manuf 224:1775–1783
31. Tao G, Ma C, Shen X, Zhang J (2017) Experimental and modeling study on cutting forces of feed direction ultrasonic vibration-assisted milling. Int J Adv Manuf Technol 90:709–715
32. Ostasevicius V, Gaidys R, Dauksevicius R, Mikuckyte S (2013) Study of vibration milling for improving surface finish of difficult-to-cut materials. J Mech Eng 59(6):351–357
33. Zemann R, Kain L, Bleicher F (2014) Vibration assisted machining of carbon fibre reinforced polymers. In: 24th DAAAM International symposium on intelligent manufacturing and automation, 2013. Procedia Eng, pp 536–543
34. Kumar MN, Subbu SK, Krishn PV, Venugopal A (2014) Vibration assisted conventional and advanced machining: a review. Procedia Eng 97:1577–1586
35. Marcel K, Marek Z, Jozef P (2014) Invesigation of ultrasonic assisted milling of aluminium alloy AlMg4.5Mn. In: 24th DAAAM International symposium on intelligent manufacturing and automation, 2013. Procedia Eng, pp 1048–1053
36. Lin SY, Kuan CH, She CH, Wang WT (2015) Application of ultrasonic assisted machining technique for glass-ceramic milling. Int J Mech Aerosp Ind Mechatron Manuf Eng 9(5):802–807
37. Ibrahim R, Rafai NH, Rahim EA, Ceng K, Ding H (2015) A performance of 2 dimensional ultrasonic vibration assisted milling in cutting force reduction, on Aluminium AL6061. ARPN J Eng Appl Sci 11(18):11124–11128
38. Zarchi MMA, Razfar MR, Abdullah A (2013) Influence of ultrasonic vibrations on side milling of AISI 420 stainless steel. Int J Adv Manuf Technol 66:83–89
39. Nath C, Rehman M (2008) Effective of machining parameters in ultrasonic vibration cutting. Int J Mach Tools Manuf 48(9):965–974
40. Mondelin A, Furet B, Rech J (2010) Characterisation of friction properties between a laminated carbon fibers reinforced polymer and a monocrystalline diamond under dry or lubricated conditions. J Tribol Int 43:1665–1673
41. Yuan S, Zhang C, Amin M, Fan H, Liu M (2015) Development of a cutting force prediction model based on brittle fracture for carbon fiber reinforced polymers for rotary ultrasonic drilling. Int J Adv Manuf Technol 81:1223–1231. https://doi.org/10.1007/s00170-015-7269-x
42. Least square method. https://en.wikiversity.org/wiki/Least-squares_Method. Accessed 15 Mar 2015